3rd Congress of Balkan Geophyiscal Society
Sofia 24-28 May, 2002. Bulgaria.

DIPOLE – DIPOLE ARRAY CONFIGURATION IN THE FRAMEWORK OF THE RECIPROCITY PRINCIPLE

A.Frasheri[1], P. Alikaj[1], N.Frasheri[2], B. Çanga[1]

[1] Polytechnic University of Tirana, Albania
[2] Institute of Informatics and Applied Mathematics, Tirana, Albania

Abstract

In the paper it is discussed the change of configuration of IP and resistivity anomalies for dipole-dipole and pole-dipole arrays. The analysis is done based on results of 2D and 3D mathematical modeling carried out successfully in the framework of scientific research of QUANTEC GEOSCIENCE Ltd.,Toronto, Ontario, Canada, and of physical modeling done in the Geophysical Laboratory "Ligor Lubonja" of the Faculty of Geology and Mining, Polytechnic University of Tirana.

Key words: dipole-dipole survey configuration, Reciprocity Principle, IP anomaly, Apparent resistivity anomaly.

Introduction

In the practice of electrical prospecting are employed various array configurations. The location of the current and potential electrodes is defined from the geological tasks to be solved. The Dipole – Dipole array is one of the most common arrays in mineral exploration. This is considered a symmetrical array in terms of the principle of reciprocity, so when the current electrodes are respectively switched with potential electrodes the same responses in IP and resistivity values are observed. However, our recent mathematical models indicate some distortions of the reciprocity principle in IP/Resistivity responses with a Dipole – Dipole array. This can lead to inaccurate target location and negative drilling results.

Presentation of Problem

The well-known reciprocity principle stands on the basis of many array configurations in electrical prospecting like Pole - Pole, Dipole - Dipole, Schlumberger, Wenner etc (Keller, G., V. and Frischknecht, F., C.,1970, Zabarovsky A. 1963, I., Frasheri, A., et al. 1985). "According to the theorem of the reciprocity, no changes will be observed in the measured voltage if the role of measuring electrodes and of the current electrodes are interchanges. Reciprocity can be readily confirmed for an electrode array over a homogeneous earth" (Keller, G., V. and Frischknecht, F., C.,1970).

There is another problem for heterogeneous mediums. Zabarovsky, A.I. (1963) shows that if a body A has received an electrical charge Q_A, a body M will have a potential U_M related with the charge Q_A following the equation:

$$U_M = \alpha_{AM} \cdot Q_A$$

where α_{AM} is a coefficient dependant on the shape of bodies A and M, their reciprocal position and the boundaries of heterogeneity. If the reversed operation would take place, i.e. the body M to receive electrical charges of Q_M then the potential U_A of the body A would be:

$$U_A = \alpha_{MA} \cdot Q_M$$

" In electrostatic phenomena science it is shown that $\alpha_{AM} = \alpha_{MA}$. If this equality is true, then $Q_M = Q_A$ and as consequence $U_M = U_A$. Translating this result in the language of electrodynamics, one may say that the potential of electrode M created by the effect of the electrode A would be equal to the potential of the electrode A, if the currents would be emitted in ground by the electrode M, with the condition that the product $I * \rho$ remains the same". On this basis he concluded that the principle of reciprocity is valid for heterogeneous mediums as well.

This conclusion is true for some arrays used for electrical surveys of apparent resistivity methods. Four electrodes Schlumberger array AMNB is reciprocal with the array MABN, pole–pole array C_1P_1 is reciprocal with P_1C_1. The pole-dipole array $P_1P_2C_1$ is reciprocal with $C_1C_2P_1$ (Frasheri, A. et al. 1985). But these reciprocities of current and receiving electrodes are not equivalent with the change of positions of couples of electrodes during profiling, in the relation to the heterogeneity. The pole-dipole array $C_1P_2P_1$ is not reciprocal with the $P_1P_2C_1$. The pole–dipole array is known as an asymmetric array. The same is for the dipole-dipole array $C_1C_2P_1P_2$ relative to $P_1P_2C_1C_2$. All this is connected with the well-known fact that pole-dipole and dipole-dipole arrays give asymmetrical anomalies for the apparent resistivity.

These changes are more evident in IP surveys. In several field surveys some asymmetrical responses are observed with a Dipole – Dipole array ($C_1C_2P_1P_2$ versus $P_1P_2C_1C_2$) in both IP and resistivity measurements. To further investigate this phenomenon some mathematical models were carried out with a program of finite element method (Frasheri A. and Frasheri N. 2000).

This analysis was initiated because of the fact that, in daily practices of geoelectrical surveys using dipole-dipole profiling a little attention is shown towards the evaluation of anomaly configuration depending on the position of couples of current and receiving electrodes. In many publications with the results of modeling and of inversion, the position of electrodes on surveying line is not shown (Dey, A., and Morrison, H. F., 1979, Tsourlos, P.I., et al., 1998, Tsourlos, P. I. and Ogilvy, R. D. 1999). This has consequences in the results of interpretation relative to spatial position of exciting bodies.

Mathematical modeling of the IP effect have based on the Bleil formulae [Bleil D., 1953; Seigel H.O., 1959]:

$$U_{IP} = c \cdot \int_V \nabla U \cdot \left(\frac{1}{\vec{R}} \right) \cdot dv \qquad (1)$$

Where: U_{ip} is the IP potential;

$\vec{R}$ is the distance vector from the integration point to the receiving point;

∇U is the potential gradient of the primary electrical field, calculated by solving the finite element model.

To achieve the mathematical modeling and the inversion of IP data, we have used the evaluation of Komarov V.A., which is expressed with the formulae [Komarov V.A., 1972]:

$$C(Uo+Uip) \approx CUo \qquad (2)$$

where: Uo is the potential of the field of primary electrical currents,
Uip is the potential of the field of induced polarization,
C is the IP susceptibility.

Based on mathematical modeling of IP anomal field, there is a formal similarity of the polarizable medium and the increasing of electrical specific resistivity of this medium as proposed by [Komarov V.A., 1972] and used by many other authors (Avdeevic M.M., Fokin A.F., Frasheri A. 1989, Frasheri et al 1994, Frasheri A., Frasheri N. 2000, Hmelevskoj V.K., Shevshin V.A. 1994, Tsourlos P.I., Szymanski J.E., Tsokas G.N., 1998, Tsourlos P.I., Ogilvy R.D., 1999):

$$\gamma^* = \gamma (1\text{-}m) \quad \text{or} \quad \rho^* = \frac{1}{\gamma(1-m)}; \qquad (3)$$

where: γ^*, ρ^* are fictive electrical conductivity and resistivity, considering the polarizability as well,
γ is electrical conductivity
m is IP chargeability

Consequently, induced polarization is considered as linear phenomenon.

For 3D modeling of IP effect from targets with massive texture in homogeneous medium we have transformed the Bleil formulae, using Green's formulae (Frasheri N. 1983, Frasheri A., Frasheri N. 2000):

$$U_{IP} = c \cdot \int_S \left(\frac{1}{R}\right) \cdot \left(\frac{dU}{dn}\right) \cdot ds \qquad (4)$$

Where: R is the distance vector from the integration point to the measurement point;
dU/dn is the gradient of the primary electrical potential on the boundary S of the target.

Ne figuren 1 tregohet rezultati i nje modelimi matematik te PP, te realizuar me anen e metodes se elementeve te fundme, i krahasuar me anomaline e vrojtuar ne terren.

With the same method of finite elements, simultaneously with the IP effect, the apparent resistivity is calculated as well.

Ne fig. 2 jepet krahasimi i anomalise se llagaritur me programin e mesiperm dhe asaj teorike si edhe anomalise se vrojtuar ne modelime fizike. Nga te dy ket raste konstatohet se saktesia e modelimit matemiatik eshte e mire.

Konceptimi i IP si fenomen linear, ka sjelle qw ne modelimet mathematike, IP anomalite e kalkuluara te ndryshojne nga ato te rezistences (fig. 3) Ne keto sections konstatohet se:

- Skaji i siperm i anomalive perputhet mire me skajin e sipert te target e polarizueshem,
- IP Anomaly mbetet e hapur drejt thellesise edhe nen skajin e poshtem te target. Ne ndryshim nga kjo, anomalia e rezistences se dukshme mbyllet nen nivelin e trupit. Te njejtin fenomen ka verejtur edhe Komarov V.A. (1972) ne IP Vertical Sounding.

Numerical results for different models

Figs. 4 and 5 present the mathematical model results of IP and resistivity responses with dipole–dipole profiling. Two anomalies are observed in both parameters. Considering the reference plotting point in between the potential electrodes P_1 and P_2, one of the anomalies is obtained over the prism while the second one at a distance O_1O_2 , between the centers of the current and potential dipoles. This presentation is conditioned on the distribution of the electrical field of the dipole - dipole array. Because a mirror image is missing in the center of the profiles, especially for IP, it means that $C_1C_2P_1P_2$ array responses are not equivalent with $P_1P_2C_1C_2$, or in mathematical terms, the principle of reciprocity is not strictly met. Keller, G., V. (1970) also presents the same phenomenon for the apparent resistivity.

In pseudosection presentation, where the plotting point is located at the intersection of lines coming at 45° from midpoints between C_1C_2 and P_1P_2, these anomalies are located in both sides of the prism (Figs. 6, 7, 8, 9). For the resistivity parameter this location is almost symmetrical in shape and amplitude, for the vertical target (Fig. 6). The symmetry is perfect in cases when the thickness of the prism is equal or greater than the dipole spacing "a", and becomes poor for thinner prisms (Fig. 9).

Alternatively, the IP anomalies are asymmetrical even in cases of vertical prisms (Fig. 6 and 9). In such cases, the epicenter of the most intensive anomaly is displaced on the side of current dipole C_1C_2. For shallow inclined prisms, the epicenters of both IP and resistivity anomalies are displaced on the opposite side of the dip. In cases of deep inclined prisms, the displacement is in the dip direction, providing that this is in the direction of the current electrodes (Fig.3).

The configuration of the IP/Resistivity anomaly is also dependent on the dip angle amplitude, relative to the current electrodes location.
The amplitude and the asymmetry of IP anomaly depend on the orientation of the polarizing vector of the primary field in connection with the prism location. In fig. 10 is presented the electric polarizing field distribution for the gradient array and dipole-dipole array. The great difference between distribution of the electric field in both cases, very well express the changes of the IP anomaly configuration for gradient and dipole-dipole array. In Fig. 11 is presented the changes of the anomaly configuration in the dependence of the location of the target, in relation with the current electrodes.

The same configuration of IP and resistivity anomalies is observed by physical modeling.

Anomalous tableau becomes more complicated when several exciting bodies are located under the surveying line. It is sufficient that the distance between two bodies to be less than 0.5 of their extension in depth, that over these bodies a single anomaly is received, being too wide and with the epicenter over the space between bodies (Fig. 12, 13). Such situation does not permit a correct interpretation of the anomaly during the inversion process. In opposite, in the real section with multiple gradient array, two separate anomalies are observed (Fig. 14).

Asymmetrical IP and resistivity anomalies, in dependence of the location of current and potential dipoles in relation with the target, shows that the lack of orientation in the current and potential electrodes is not always without problems in manual or inversion interpretations of the IP/Resistivity data surveyed with a dipole–dipole array.

Conclusions

1. The anomaly configuration in an IP/Resistivity survey with a dipole–dipole array is dependent on the location of the current and potential electrodes in connection to target. In this regard, logistical information about the survey should include the array orientation (left-array or right-array). The position of the array must be shown in plots and pseudosections. During the profiling, it is necessary to keep the same configuration of current and receiving dipoles.

2. The results of the survey should be interpreted accordingly the array orientation in the survey line, in order to define the placement of exciting bodies, the direction of its inclination and the its depth. The same recommendation is valid for the process of inversion.

3. Profiling with dipole-dipole arrays has smaller discriminative capability for IP surveys, compared with other arrays as the gradient array.

References

Alikaj, P., 1978. IP vertical section method modeling, observed by multiple gradient arrays. Album, Chair of Geophysics, Faculty of Geology and Mining, Polytechnic University of Tirana, Albania.

Avdeevic, M. M.,1 Fokin A. F., 1992. Electrical Modeling of Geophysical Potential Fields. Publishing House Njedra, Sankt Peterburg, (in Russian).

Bleil, D., 1953. Induced Polarization: a method for geophysical prospecting; Geophysics, 18, pp. 636-662.

Dey, A., Morrison, H. F., 1979. Resistivity modeling for arbitrarily shaped three-dimensional structures. Geophysics, v0;. 34, No. 4.

Frasheri, A., Avxhiu, R., Malaveci, M., Alikaj, P., Leci, V., Gjovreku, V., 1985. Electrical Prospecting. Tirana University Publishing House. Tirana, Albania.

Frasheri, A., 1989. An algorithm for mathematical modeling of anomalous effect of Induced Polarization over rich copper ore bodies with any geometric shape. Bulletin of Geological Sciences (Tirana) No. 1, pp.116 - 126, (in Albanian, summary English).

Frasheri, A., Tole, Dh., Frasheri, N., 1994. Finite element modeling of induced polarization

electric potential field propagation caused by ore bodies of any geometrical shape, in mountainous relief. Commun. Fac. Sci., Univ. Ank. Serie C. V. 8, pp. 13-26 (1990).

Frasheri, A., Lubonja, L. Alikaj, P., 1995. On the application of geophysics in the exploration for copper and chrome ores in Albania. Geophysical Prospecting, 1995, 43, pp. 743-757.

Frasheri, A. Frasheri, N., 2000. Finite element modeling of IP anomalous effect from ore bodies of any geometrical shape located in rugged relief area. Journal of Balkan Geophysical Society. No. 1, 2000, pp.3-6.

Frasheri, N., 1983. "Two Superparametric 4-node Elements to solve Elliptic Equations in Infinite Domains". Bulletin of Natural Sciences 1, 17-23. University of Tirana, (In Albanian, abstract in French).

Hmelevskoj V.K., Shevshin V.A., 1994. Elektrorazvjedka metodom soprotivlenia. Izdatelstvo Moskovskogo Universiteta, Moskva.

Keller, G., V., and Frischknecht, F., C., 1970. Electrical Methods in Geophysical Prospecting. Pergamon Press, Oxford, New York, Toronto, Sydney, Braunsckweig.

Komarov, V.A., 1972. Electrical Prospecting for Induced Polarization Method. Published by Njedra, (in Russian).

Langore, L., Alikaj, P., and Gjovreku, Dh. 1989. Achievements in copper exploration in Albania with IP and EM methods: Geophysical Prospecting, 37, pp. 975-991.

Lubonja, L., Frasheri, A., 1965. Induced Polarization method and its application for sulphide ore exploration. University of Tirana Publishing House (in Albanian).

Lubonja, L., Frasheri, A., Avxhiu, R., Duka, B., Alikaj, P., Bushati, S. 1985. Some trends in the increasing of the depth of geophysical investigation for ore deposits. Bulletin of Geological Sciences (Tirana) No. 3, pp. 33 - 52, (in Albanian, summary English).

Seigel, H.O., 1959. Mathematical formulation and type curves for Induced Polarization. Geophysics, 37, pp. 547-565.

Tsourlos, P.I., Szymanski, J.E., Tsokas G.N., 1998. Smoothness constrained algorithm for the fast 2-D inversion of DC resistivity and induced polarization data. Journal of BalcanGeophysical Society, Vol. 1, Numbers 1, pp 3-14.

Tsourlos, P.I., Ogilvy, R.D., 1999. An algorithm for the 3-D inversion of topographic resistivity and induced polarization data: Preliminary results. Journal of Balkan Geophysical Society, Vol. 2, Numbers 1, pp 30-46.

Zabarovskyy, A., I., 1963. Electrorazvyedka. Geoltehyzdat, Moscow.

Zienkiewicz, O., 1977. The Finite Element Method. McGraw Hill London.

LIST OF CAPTIONS

Fig. 1. A finite element section of IP an irregular body over a rugged relief.

Fig. 2. IP profiling over a prism: Theoretical, calculated and physical modeling.

Fig. 3. IP and Ro Realsections with multiple gradient arrays. Mathematical model.
Model: horizontal prism at depth 2 Dx, dimensions of the prism 1 x 1 x 20 Dx. Prism Resistivity 2 000 Ohmm, IP Chargeability 100 mV/V, Environment Resistivity 1 000 Ohmm , IP Chargeability 1 mV/V.

Fig. 4. IP and Resistivity mathematical modeling. Dipole-dipole profiling, C_1C_2-P_1P_2=1 Dx, n=16 Dx.
Model: 2D horizontal prism at depth 5 Dx, dimensions of the prism section 2 x 2 Dx. Resistivity of the prism 1 Ohmm, IP Chargeability 500 mV/V, Resistivity of the environment 1 000 Ohmm, IP Chargeability of the environment 0.01 mV/V.

Fig. 5. IP and Resistivity mathematical modeling. Dipole-dipole profiling. C_1C_2-P1P2=2 Dx, n=1-10 Dx.

Model: 2D vertical prism at depth 1 Dx, dimensions of the prism section 2 x 9 Dx. Resistivity of the prism 20 000 Ohmm, IP Chargeability 500 mV/V, Resistivity of the environment 1 000 Ohmm, IP Chargeability of the environment 0.01 mV/V.

Fig. 6. IP and Resistivity Pseudosection with dipole-dipole array. C_1C_2-P_1P_2=1 Dx, n=1-11 Dx.

Mathematical model: 2D vertical prism at depth 2 Dx, dimensions of the prism section 1 x 2 Dx. Resistivity of the prism 1 Ohmm, IP Chargeability 300 mV/V, Resistivity of the environment 100 Ohmm, IP Chargeability of the environment 0.01 mV/V.

Fig. 7. IP and Resistivity Pseudosection with dipole-dipole array, C_1C_2-P_1P_2=1 Dx, n=1-11 Dx.

Mathematical model: 2D inclined prism at depth 2 Dx, dimensions of the prism section 1 x 2 Dx. Resistivity of the prism 1 Ohmm, IP Chargeability 300 mV/V, Resistivity of the environment 100 Ohmm, IP Chargeability of the environment 0.01 mV/V.

Fig. 8. IP and Resistivity Pseudosection with dipole-dipole array, P_1P_2-$C_1C_{2=}$1 Dx, n=1-11 Dx.

Mathematical model: 2D inclined prism at depth 2 Dx, dimensions of the prism section 1 x 2 Dx. Resistivity of the prism 1 Ohmm, IP Chargeability 300 mV/V, Resistivity of the environment 100 Ohmm, IP Chargeability of the environment 0.01 mV/V.

Fig. 9. IP and Resistivity Pseudosection witj dipole-dipole array, C_1C_2-P_1P_2=1 Dx, n=1-11 Dx.

Mathematical model: 2D vertical prism at depth 1 Dx, dimensions of the prism section 4 x 50 Dx. Resistivity of the prism 3 Ohmm, IP Chargeability 50 mV/V, Resistivity of the environment 1 000 Ohmm, IP Chargeability of the environment 0.01 mV/V.

Fig. 10. Realsection of the potential of polarizing electric field (Uo) of transmitting gradient array. AB_{max} = 30 Dx (a) and of transmitting dipole C_1C_2 = 1 Dx.

Mathematical model: Vertical prism. Dimensions of the prism 2 x 30 x 20 Dx, Resistivity of the prism 20 000 Ohmm, Resistivity of the environment 1 000 Ohmm.

Fig. 11. Dependence of IP anomalies configuration from location of the target.

Mathematical model: Vertical prism.

Fig. 12. IP Realsection with multiple gradient arrays.

IP contour interval 2 mV/V.

Mathematical Model: Two parallel inclined prisms (dip=70°) at depth 5 Dx, dimensions of the prisms 1 x 20 x 20 Dx. Distance between the prisms 10 Dx, Prisms Resistivity 2 000 Ohmm, IP Chargeability 500 mV/V, Environment Resistivity 500 Ohmm , IP Chargeability 1 mV/V.

Fig. 13. IP Pseudosection with dipole-dipole array, C_1C_2=P_1P_2=1 Dx, n=1-39.

Mathematical Model: Two parallel inclined prisms (dip=70°) at depth 5 Dx, dimensions of the prisms 1 x 20 x 20 Dx. Distance between the prisms 10 Dx, Prisms Resistivity 2 000 Ohmm, IP Chargeability 500 mV/V, Environment Resistivity 500 Ohmm , IP Chargeability 0.01 mV/V.

Fig. 14. IP Pseudosection with dipole-dipole array, P_1P_2=C_1C_2=1 Dx, n=1-39.

Mathematical Model: Two parallel inclined prisms (dip=70°) at depth 5 Dx, dimensions of the prisms 1 x 20 x 20 Dx. Distance between the prisms 10 Dx, Prisms Resistivity 2 000 Ohmm, IP Chargeability 500 mV/V, Environment Resistivity 500 Ohmm , IP Chargeability 0.01 mV/V.
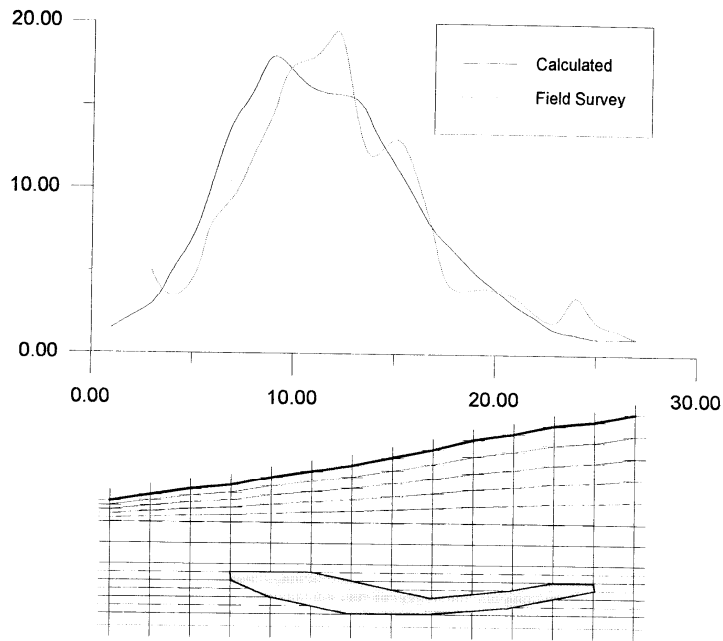
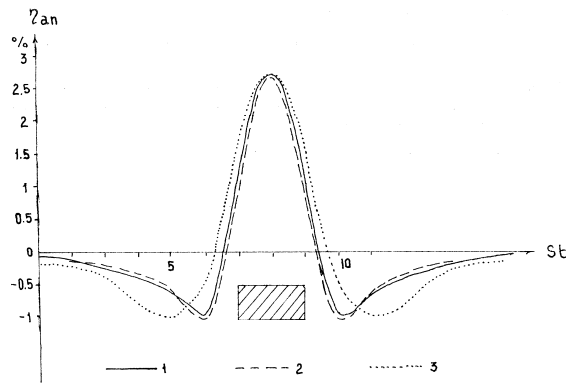Fig. 1. A finite element section of IP an irregular body over a rugged relief.

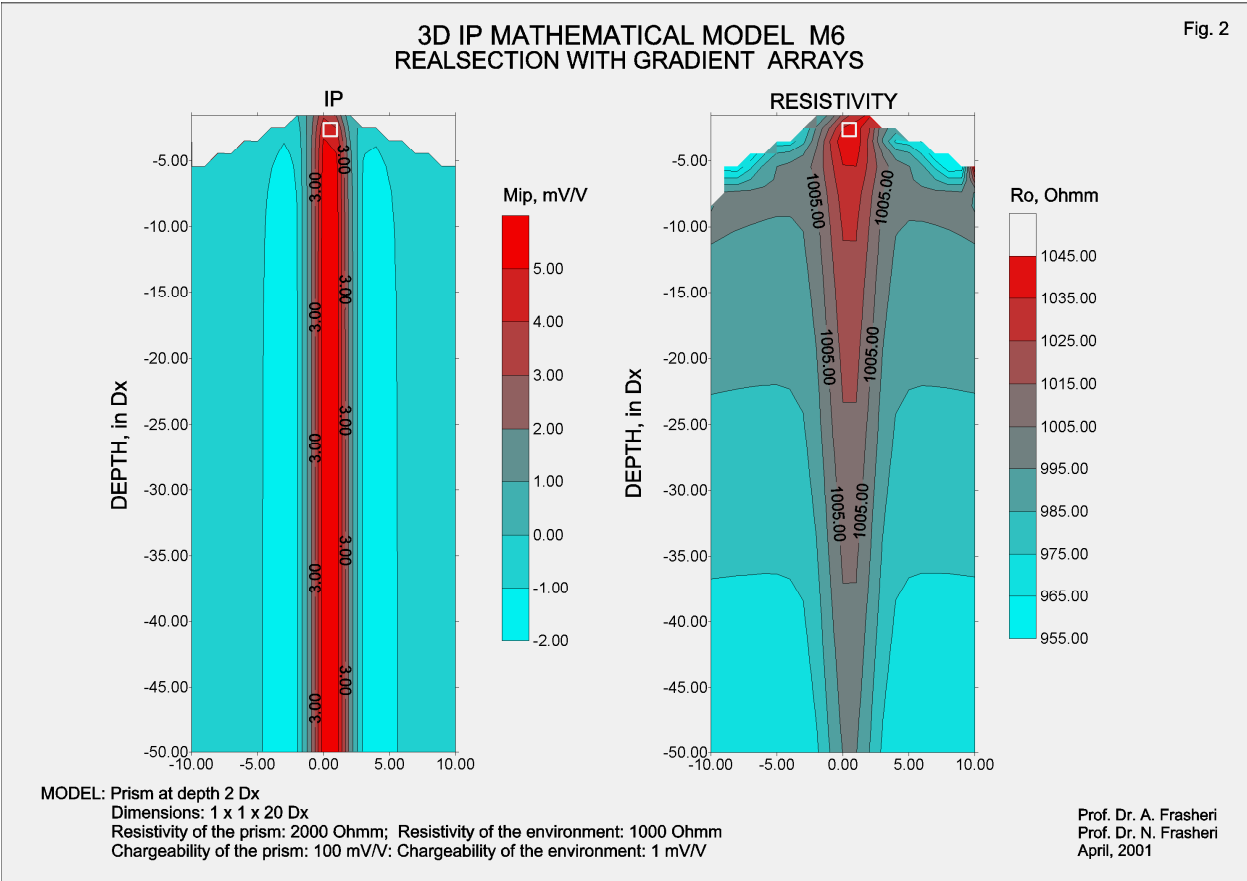Fig. 2. IP profiling over a prism: Theoretical, calculated and physical modeling.

Fig. 3. IP and Ro Realsections with multiple gradient arrays. Mathematical model.
Model: horizontal prism at depth 2 Dx, dimensions of the prism 1 x 1 x 20 Dx. Prism Resistivity 2 000 Ohmm, IP Chargeability 100 mV/V, Environment Resistivity 1 000 Ohmm , IP Chargeability 1 mV/V.
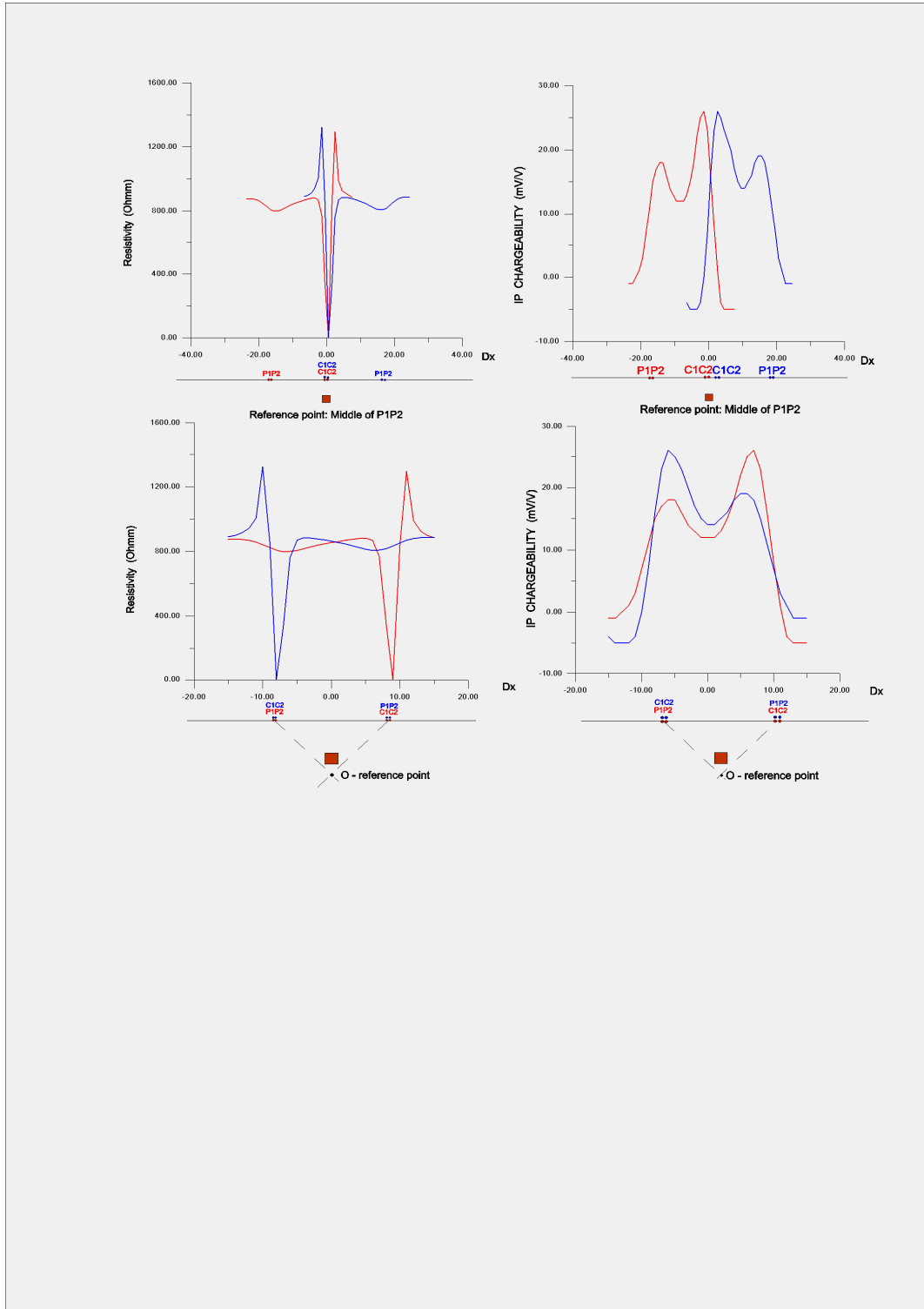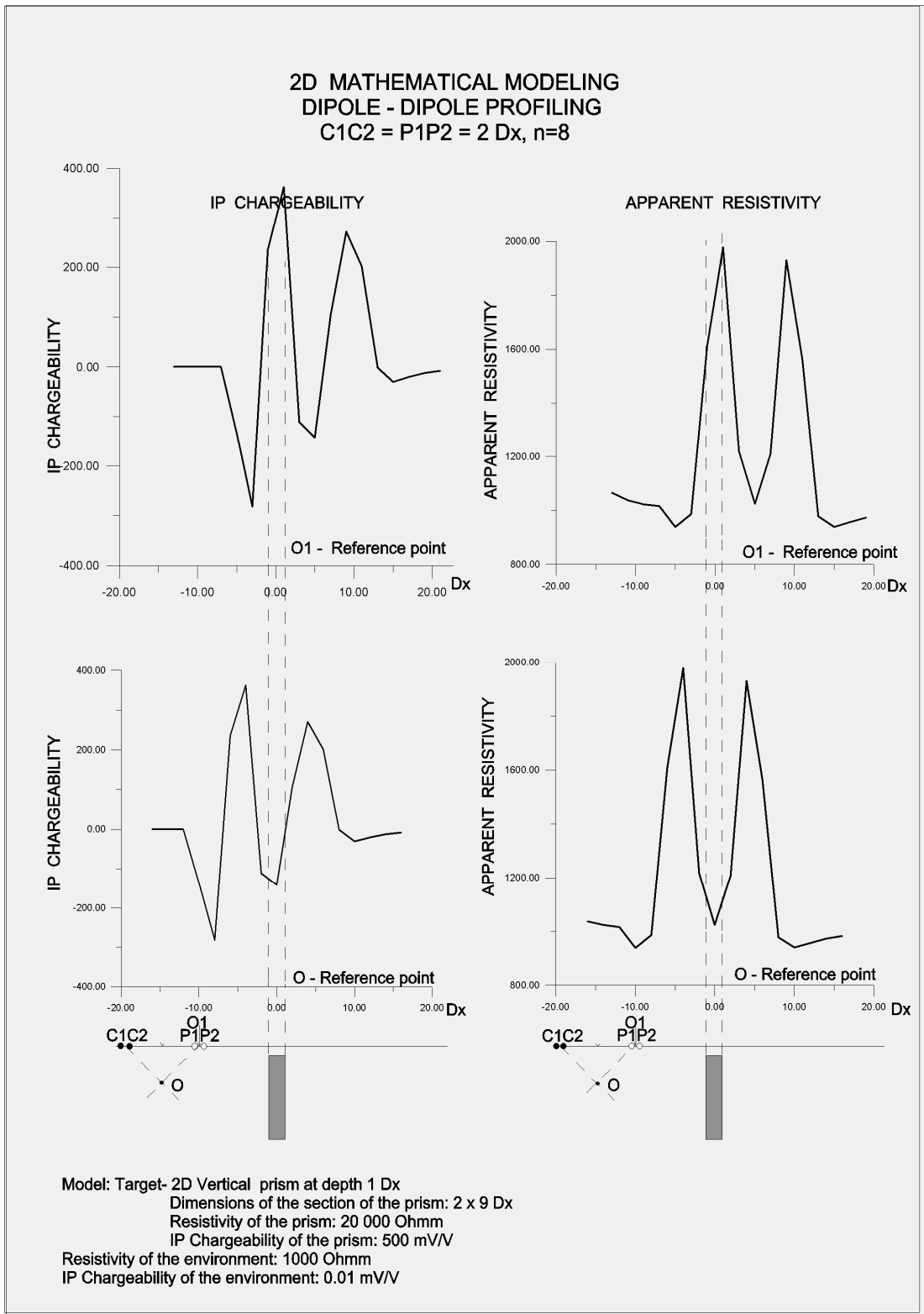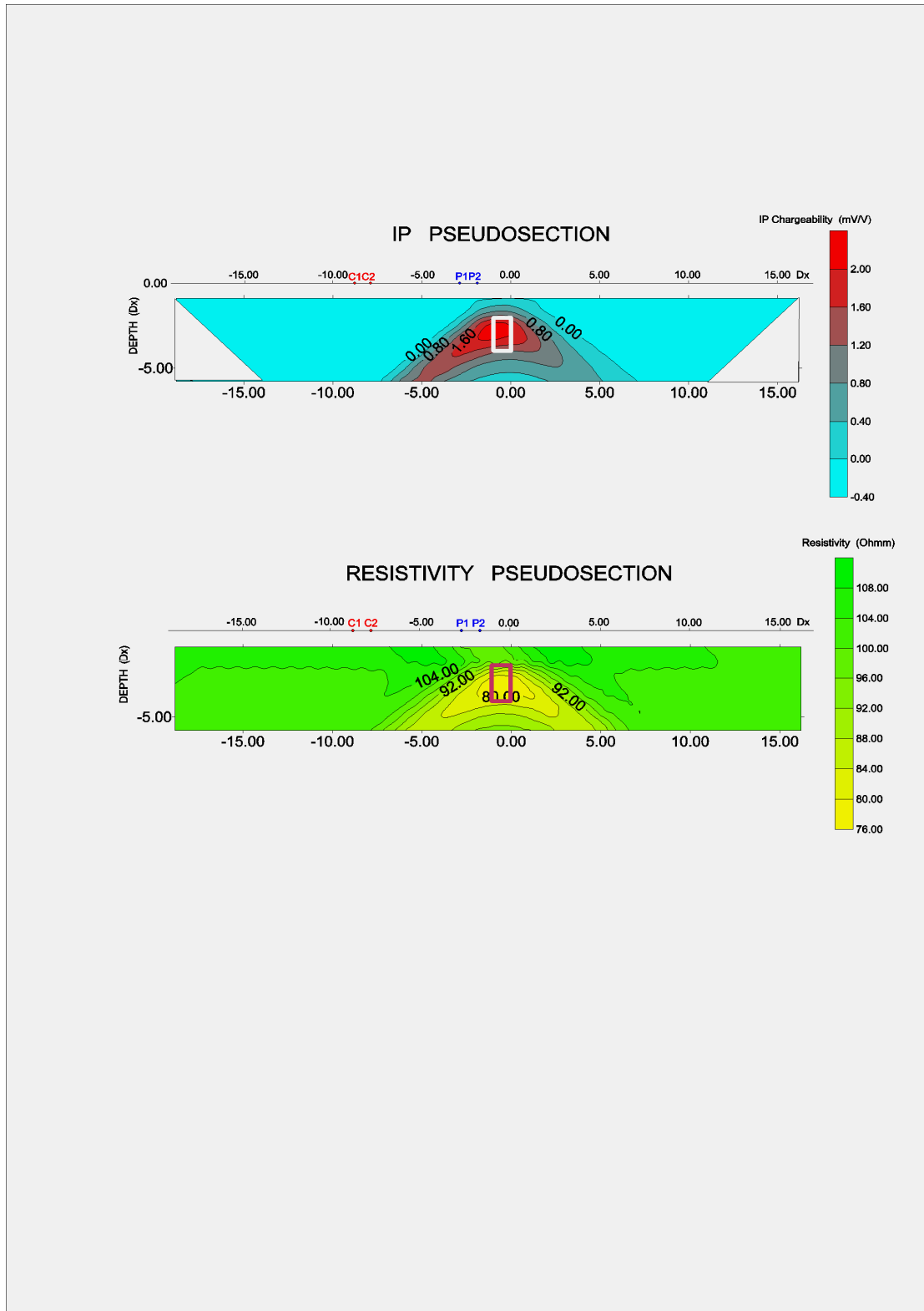
Fig. 4. IP and Resistivity mathematical modeling. Dipole-dipole profiling, C_1C_2-P_1P_2=1 Dx, n=16 Dx.
Model: 2D horizontal prism at depth 5 Dx, dimensions of the prism section 2 x 2 Dx.
Resistivity of the prism 1 Ohmm, IP Chargeability 500 mV/V, Resistivity of the environment 1 000 Ohmm, IP Chargeability of the environment 0.01 mV/V.
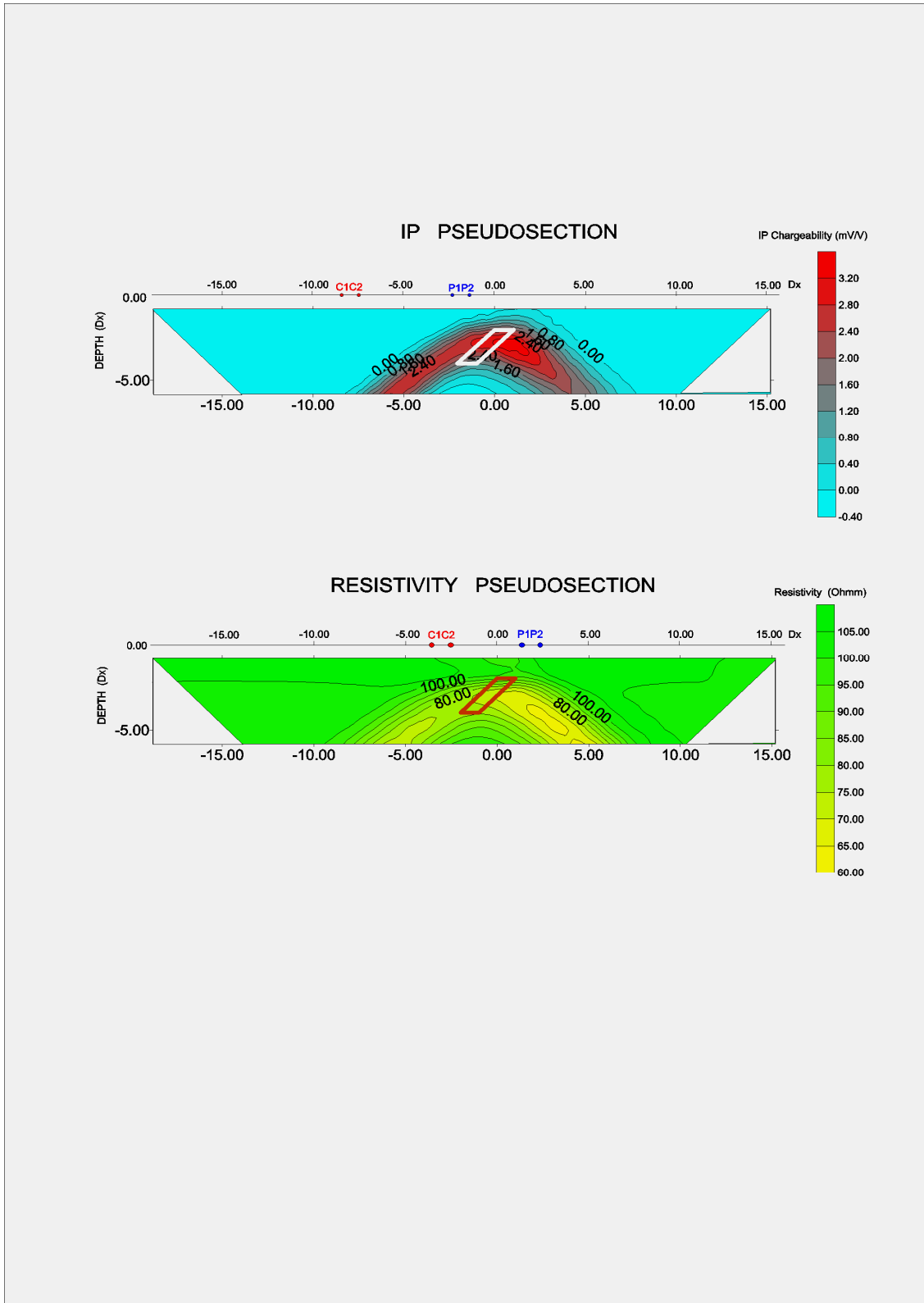
Fig. 5. IP and Resistivity mathematical modeling. Dipole-dipole profiling. C_1C_2-P1P2=2 Dx, n=1-10 Dx.
Model: 2D vertical prism at depth 1 Dx, dimensions of the prism section 2 x 9 Dx. Resistivity of the prism 20 000 Ohmm, IP Chargeability 500 mV/V, Resistivity of the environment 1 000 Ohmm, IP Chargeability of the environment 0.01 mV/V.
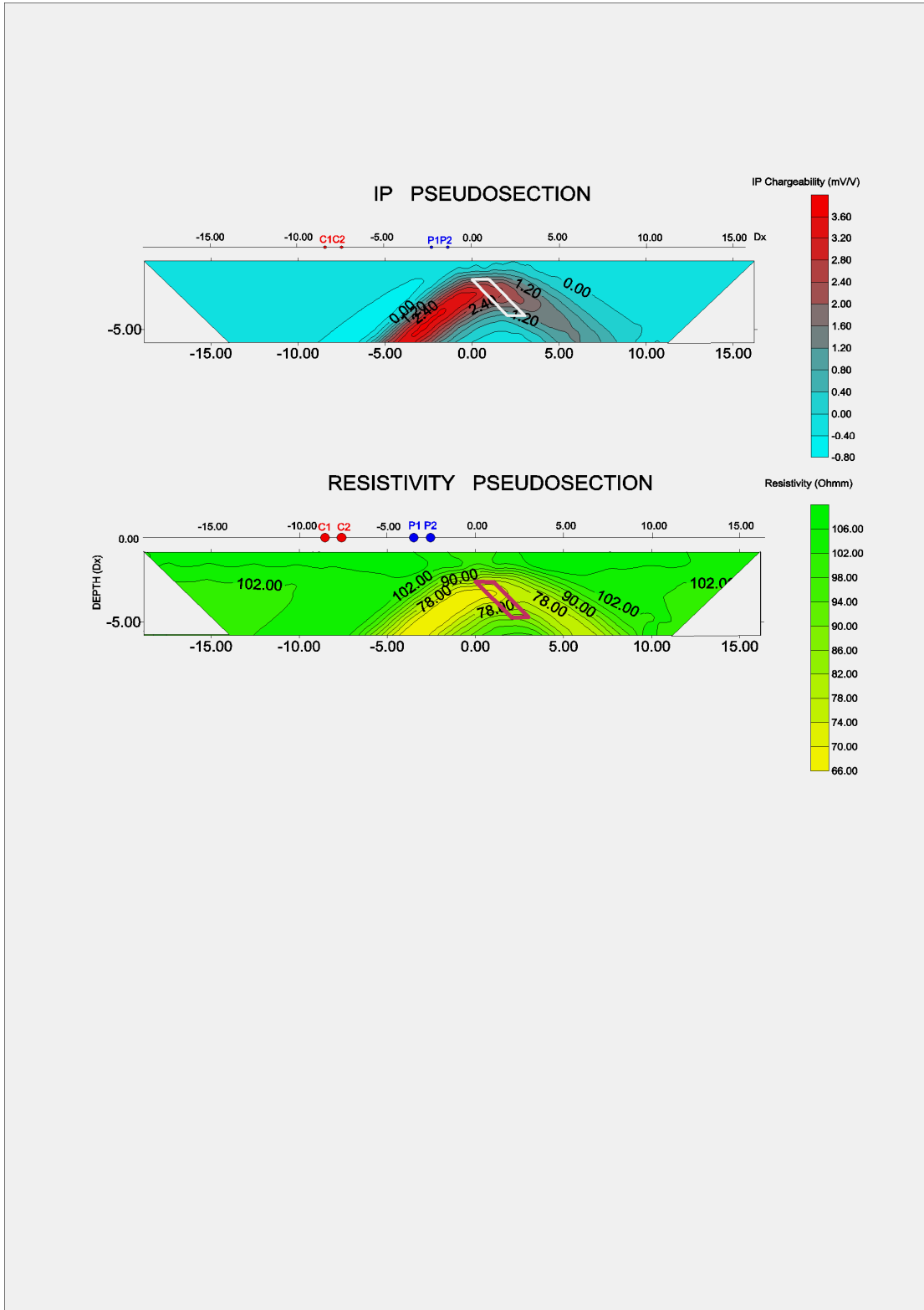
Fig. 6. IP and Resistivity Pseudosection with dipole-dipole array. C_1C_2-P_1P_2=1 Dx, n=1-11 Dx. Mathematical model: 2D vertical prism at depth 2 Dx, dimensions of the prism section 1 x 2 Dx. Resistivity of the prism 1 Ohmm, IP Chargeability 300 mV/V, Resistivity of the environment 100 Ohmm, IP Chargeability of the environment 0.01 mV/V.
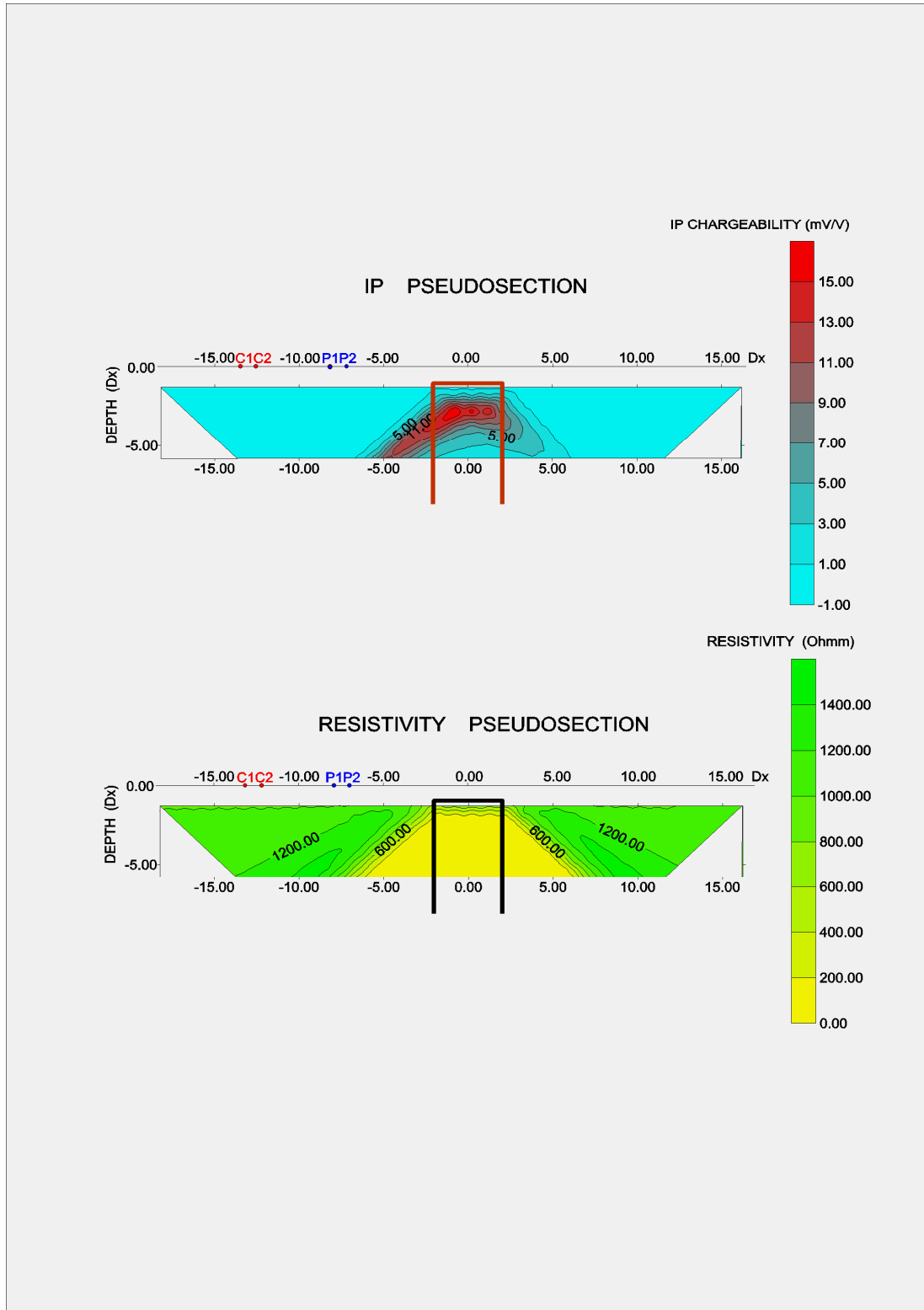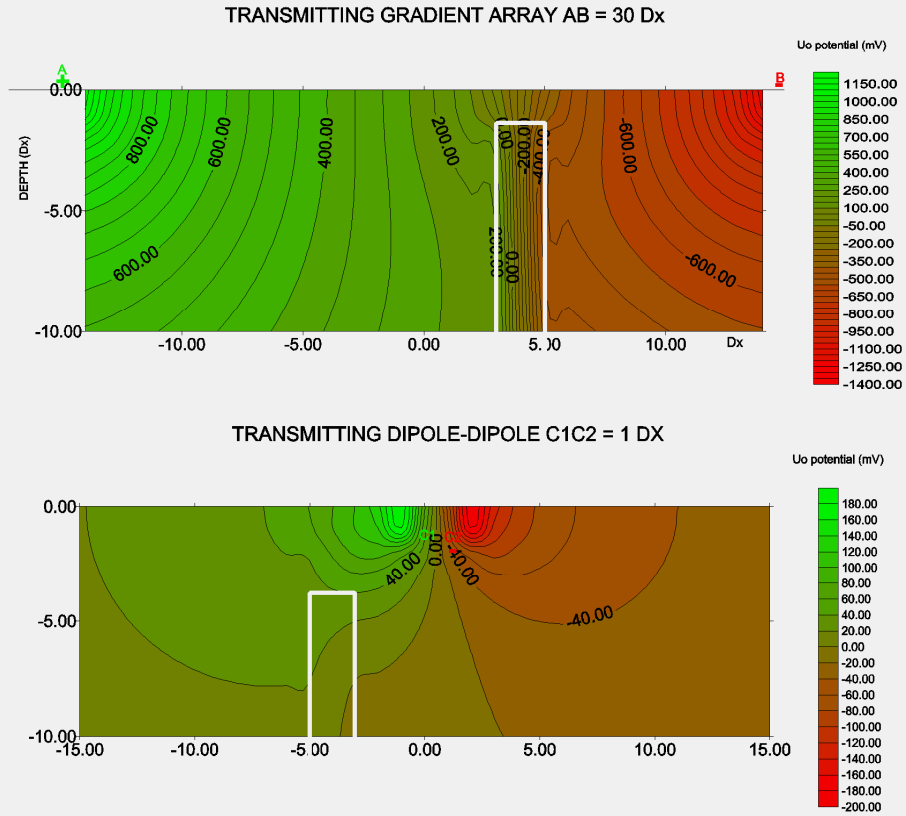
Fig. 7. IP and Resistivity Pseudosection with dipole-dipole array, $C_1C_2-P_1P_2=1$ Dx, n=1-11 Dx. Mathematical model: 2D inclined prism at depth 2 Dx, dimensions of the prism section 1 x 2 Dx. Resistivity of the prism 1 Ohmm, IP Chargeability 300 mV/V, Resistivity of the environment 100 Ohmm, IP Chargeability of the environment 0.01 mV/V.

Fig. 8. IP and Resistivity Pseudosection with dipole-dipole array, P_1P_2-C_1C_2=1 Dx, n=1-11 Dx. Mathematical model: 2D inclined prism at depth 2 Dx, dimensions of the prism section 1 x 2 Dx. Resistivity of the prism 1 Ohmm, IP Chargeability 300 mV/V, Resistivity of the environment 100 Ohmm, IP Chargeability of the environment 0.01 mV/V.

Fig. 9. IP and Resistivity Pseudosection witj dipole-dipole array, C_1C_2-P_1P_2=1 Dx, n=1-11 Dx. Mathematical model: 2D vertical prism at depth 1 Dx, dimensions of the prism section 4 x 50 Dx. Resistivity of the prism 3 Ohmm, IP Chargeability 50 mV/V, Resistivity of the environment 1 000 Ohmm, IP Chargeability of the environment 0.01 mV/V.

15

2D RESISTIVITY MATHEMATICAL MODELING
REAL - SECTION OF THE POTENTIAL OF POLARIZING
ELECTRIC FIELD (Uo)

Fig. 10. Realsection of the potential of polarizing electric field (Uo) of transmitting gradient array. AB_{max} = 30 Dx (a) and of transmitting dipole C_1C_2 = 1 Dx.

Mathematical model: Vertical prism. Dimensions of the prism 2 x 30 x 20 Dx, Resistivity of the prism 20 000 Ohmm, Resistivity of the environment 1 000 Ohmm.
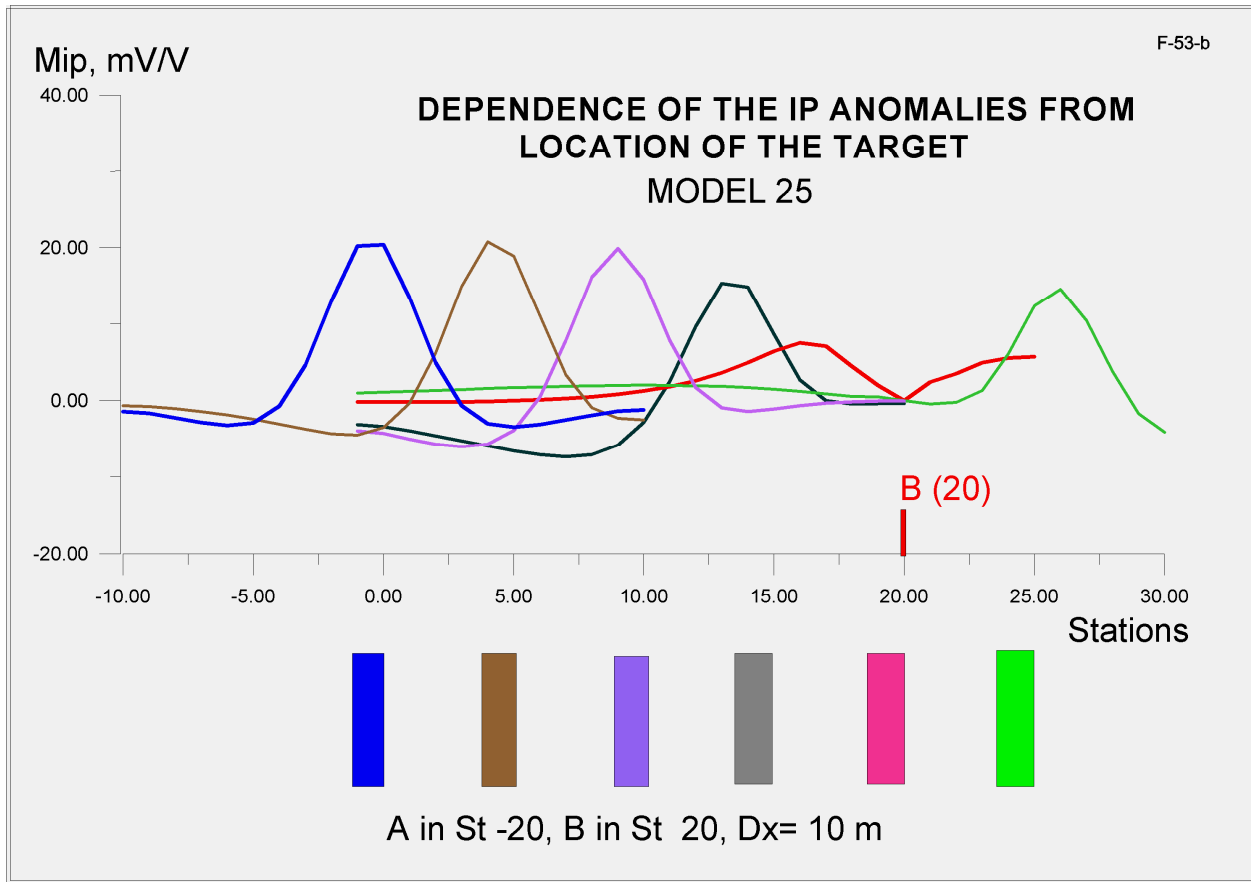
Fig. 11. Dependence of IP anomalies configuration from location of the target.
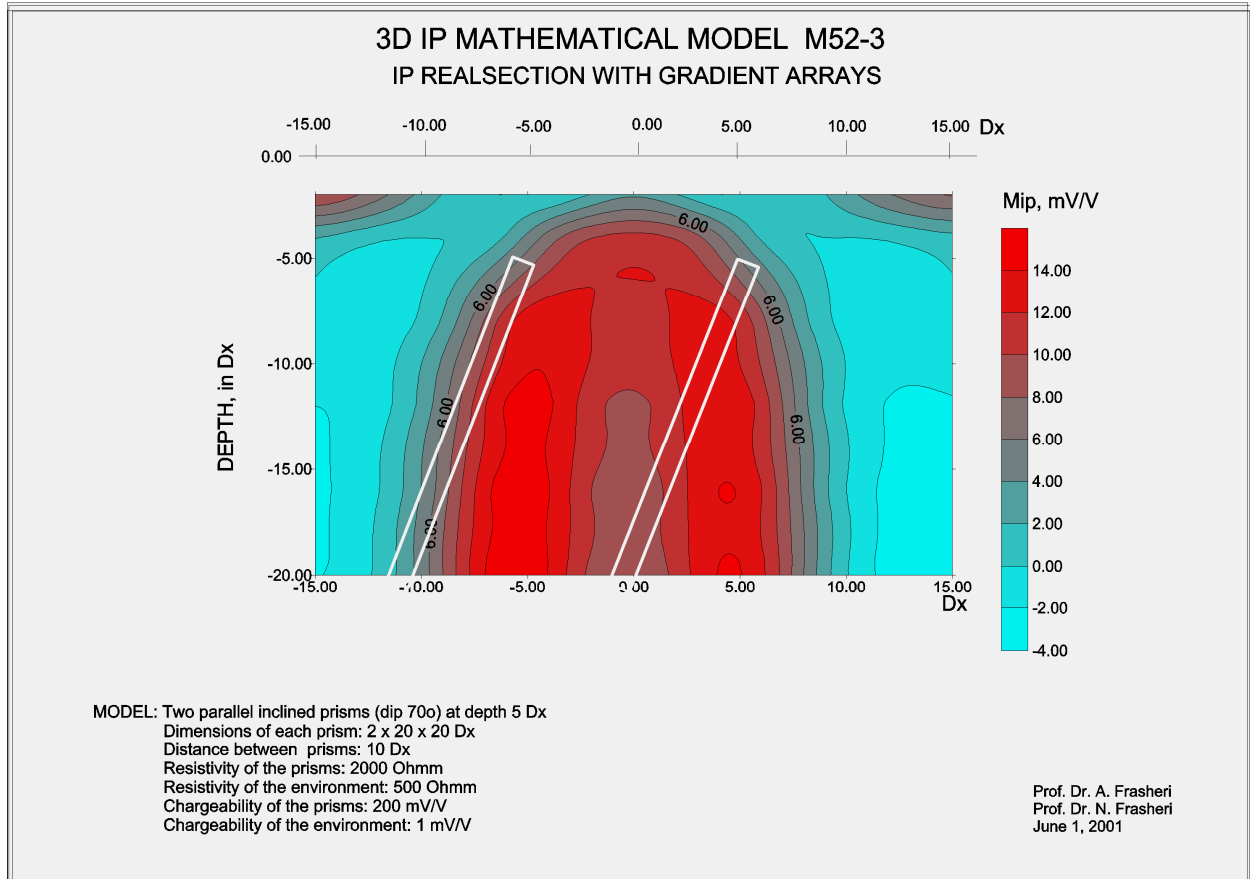Mathematical model: Vertical prism.

Fig. 12. IP Realsection with multiple gradient arrays.
IP contour interval 2 mV/V.
Mathematical Model: Two parallel inclined prisms (dip=70°) at depth 5 Dx, dimensions of the prisms 1 x 20 x 20 Dx. Distance between the prisms 10 Dx, Prisms Resistivity 2 000 Ohmm, IP Chargeability 500 mV/V, Environment Resistivity 500 Ohmm , IP Chargeability 1 mV/V.
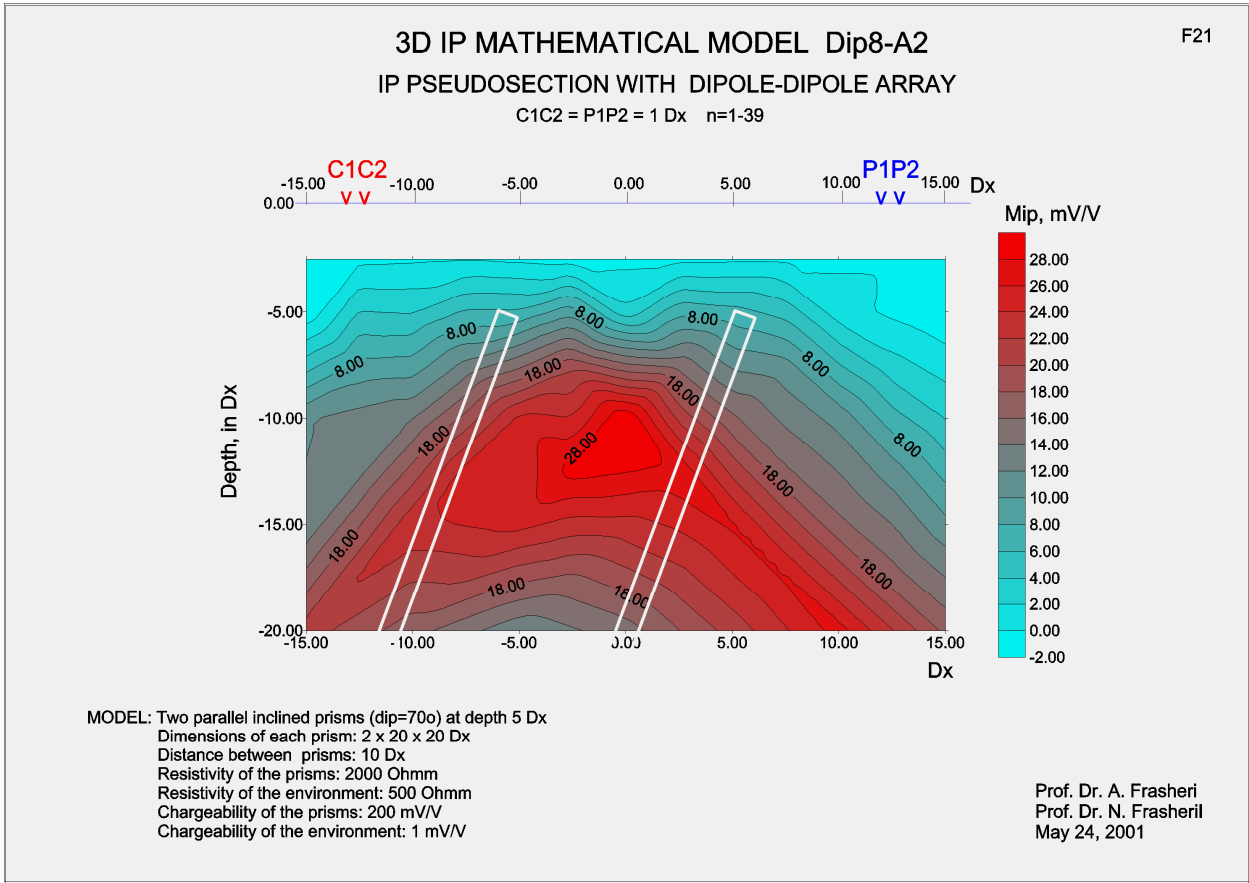
Fig. 13. IP Pseudosection with dipole-dipole array, $C_1C_2=P_1P_2=1$ Dx, n=1-39.

Mathematical Model: Two parallel inclined prisms (dip=70°) at depth 5 Dx, dimensions of the prisms 1 x 20 x 20 Dx. Distance between the prisms 10 Dx, Prisms Resistivity 2 000 Ohmm, IP Chargeability 500 mV/V, Environment Resistivity 500 Ohmm , IP Chargeability 0.01 mV/V.
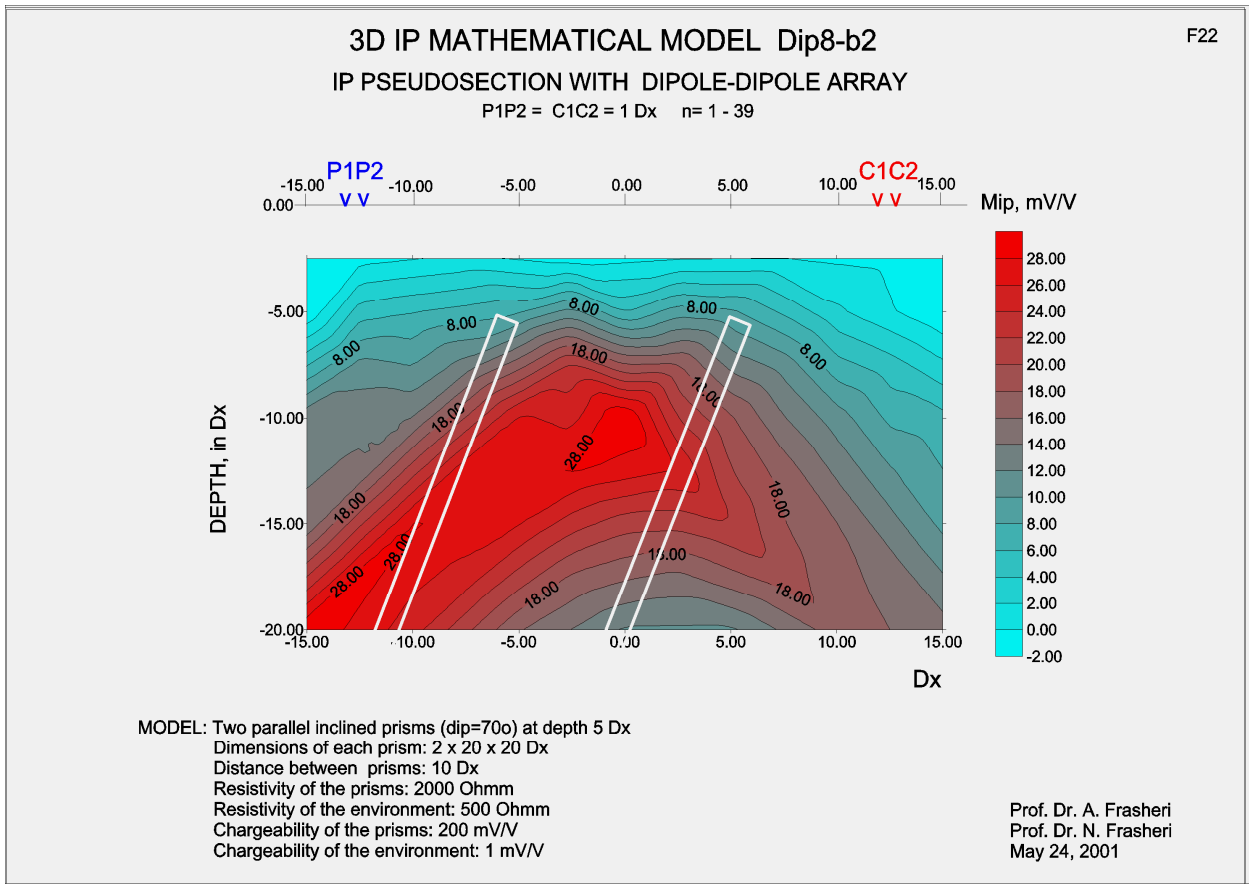
Fig. 14. IP Pseudosection with dipole-dipole array, $P_1P_2=C_1C_2=1$ Dx, n=1-39.
Mathematical Model: Two parallel inclined prisms (dip=70°) at depth 5 Dx, dimensions of the prisms 1 x 20 x 20 Dx. Distance between the prisms 10 Dx, Prisms Resistivity 2 000 Ohmm, IP Chargeability 500 mV/V, Environment Resistivity 500 Ohmm , IP Chargeability 0.01 mV/V.